Indium free and flexible organic solar cell

ARTICLE · JANUARY 2015

READS
116

5 AUTHORS, INCLUDING:

M. Makha
Empa - Swiss Federal Laboratories for Mate…
19 PUBLICATIONS **79** CITATIONS
SEE PROFILE

Benchouk Kheireddine
University of Oran
17 PUBLICATIONS **106** CITATIONS
SEE PROFILE

Technology Letters, Vol.2, No.3(2015) 5-11
ISSN: 2348-8131
Available online at www.technologyletters.us

Indium free and flexible organic solar cells

K. El Assad Zemallach Ouari[1], B. Kouskoussa[1], M. Makha[2], K. Benchouk[1], A. Khelil[1].

[1] *Université d'Oran 1 — Ahmed Ben Bella, LPCMME, BP 1524 ELM Naouer 31000 Oran, Algeria.*
[2] *Université Ibn Tofail, LOPCM, Faculté des sciences BP 133 Kenitra 14000, Marocco*

Abstract
The energy conversion efficiency of indium free flexible organic solar cells based on simple planar CuPc/C_{60} heterojunction is studied as a function of the anode free properties. The free indium anode consists in a MoO_3/Ag/MoO_3 multilayer structure. It is shown that the efficiency of the cells is optimized when the Ag film thickness is increased from 11nm to 17 nm. Moreover the best efficiency are achieved when a double anode buffer layer, Au/CuI is introduced between the MoO_3/Ag/MoO_3 electrode and the CuPc organic layer. Such behaviours are interpreted with the help of a equivalent electrical circuit of the cells. It is shown that, when deposited onto very thin flexible plastic substrate the properties of the MoO_3/Ag/MoO_3 electrodes are degraded during the realisation of the cell, which justifies the need of thicker Ag film and of the ultra tin Au film.

Keywords: Organic solar cells, Indium free, Flexibility, Electrical modelling.

Corresponding author: K. El Assad Zemallach Ouari: houari.kadda@yahoo.fr

1 Introduction

Organic solar cells have attracted a strong interest during the last twenty years. Among the most important advantages of such cells are their possible flexibility and lightweight.
The hearth of these cells is based on a heterojunction electron donor/electron acceptor (ED/EA). Two organic solar cell families are encountered, that using on a polymer as electron donor and that using small molecules. Both of them use, nearly systematically, indium tin oxide (ITO) as transparent electrode. As a matter of fact, when adaptated to the band sturcture of the active layer by introducing buffer layer between ITO and the organic film, it allows the cells to achieve their highest power conversion efficiency. However, ITO is not without some disadvantages, mainly in the case of flexible substrate. Not only In is scarce, but also, ITO is quite brittle, which is not suitable for flexible optoelectronic devices. Then, it is necessary to look for flexible and In free new transparent conductive electrode (TCE) [1-4]. Among the possible alternatives, the multilayers structures, dielectric/metal/dielectric (DMD) answer adequately to the necessity of conductivity, transparency and flexibility [1, 5]. Ag is the metal giving the highest performances due to its high conductivity and its low absorption in the visible. Oxides of metal transition are often used as dielectric due to their high refractive index. For instance, after optimisation of the thickness and deposition rate of the different films, MoO_3/Ag/MoO_3 (MAM) multilayer

structures were efficiently employed as alternative transparent conductive electrodes [6]. Following the optimisation of these MAM structures on glass substrates, this investigation was extended to the realisation of TCE onto flexible substrates [7]. Unfortunately, not only the efficiency of the cells is quite poor, but also it is smaller than that obtained with ITO deposited onto flexible substrate. In the present manuscript, in order to understand the origin of these disappointing results, we confront these experimental results to a theoretical modelling, using different equivalent electrical circuits for the cells. As a matter of fact, an equivalent electrical circuit model could be helpful in understanding the behaviour of MAM electrodes by providing a quantitative estimation for losses in the cells.

2 Experimental

The organic photovoltaic cells (OPVCs) probed in the present work, were small molecules planar heterojunctions. They are classically based on an organic bilayer sandwiched between two electrodes. One of these electrodes must be transparent and the other must be highly reflexive. The bilayer is a heterojunction between the electron donor (ED) and the electron acceptor (EA). About the electrodes, while aluminum is often used as reflexive cathode, the transparent conductive anode is usually the indium tin oxide (ITO). However, in the present work, the MAM indium free TCE was used as anode. ITO anode was used as reference anode. As usual in such structures, an anode buffer layer (ABL) and a cathode buffer layer (CBL) were necessary to achieve performing OPVCs [6].
The structures were deposited on 50µm-thick polyethylene terephthalate (PET) substrates. The MAM multilayer structures were deposited by sequential evaporation without breaking the vacuum (10−4 Pa). Deposition rate and film thickness were measured in situ by a quartz monitor. It was already shown that, when deposited onto PET substrates, the optimum film thicknesses are: MoO_3 (20 nm)/Ag (11 nm)/MoO_3 (35 nm) [7]. The deposition rate of MoO3 was 0.05 nm/s, while the silver deposition rate was 0.3 nm/s [6].
The organic donor/acceptor couple used is copper phthalocyanine (CuPc)/fullerene (C_{60}), the ABL is, CuI [8], while the CBL is the aluminium tris(8-hydroxyquinoline) (Alq_3). The CuI, C_{60}, CuPc, Alq_3 films were successively sublimated under vacuum and finally the metal anode was evaporated on the top of the device giving the following inverted OPVC: MAM/CuI (3 nm)/ CuPc (35 nm)/ C_{60} (40 nm)/ Alq_3 (6 nm)/ Al (120 nm). Sometimes, a thin (0.5 nm) film of Au was introduced between the MAM structure and the CuI layer [9]. The top electrode was deposited through a mask with 2x10 mm^2 active area.
The characteristics of the photovoltaic cells were measured using a calibrated solar simulator (Oriel 300 W) at 100 mW/cm2 light intensity adjusted with a reference cell (0.5 cm2 CIGS solar cell,). Measurements were performed at ambient atmosphere. All devices were illuminated through the transparent electrode.

3 Experimental results

Typical J–V characteristics under one sun global AM 1.5 simulated solar illumination, of cells with MAM anodes are presented in Fig. 1. The corresponding photovoltaic performance data of cells, achieved under AM1.5 conditions are reported Table 1.

Technology Letters, Vol.2, No.3(2015) 5-11
ISSN: 2348-8131
Available online at www.technologyletters.us

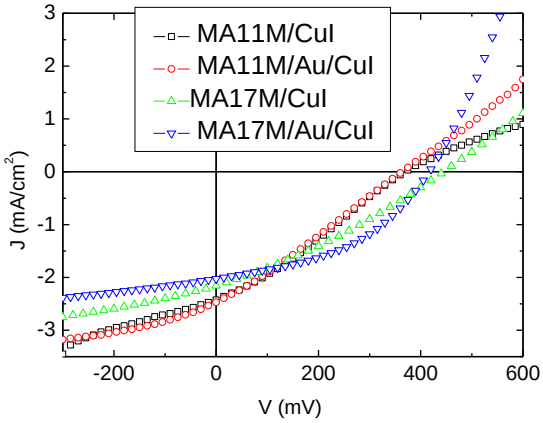

Figure 1: J-V characteristics of OPVCs with different anodes.

Since the performances of the MAM, when deposited onto PET, where quite faint when used as anode, we try to improve them by increasing the Ag film thickness. We can see in Figure 1 and table 1 that the increase of the Ag film thickness allows improving the performances of the OPVCs. It can also be seen that the introduction of an ultra thin Au film permits to optimise the performance of the OPVC, when the Ag film thickness is 17 nm.

Anode/ABL	Voc (V)	Jsc (mA/cm^2)	FF (%)	η (%)
MA(11)M/CuI	0.37	2.4	29	0.26
MA(11)M/Au/CuI	0.36	2.4	31	0.26
MA(17)M/CuI	0.44	2.15	35	0.32
MA(17)M/Au/CuI	0.43	2.1	43	0.37

Table 1: OPVCs performances variation with the anode configuration.

It can be seen in figure 1 that the shape of the J-V curves depends on the Ag film thickness. Only the curve obtained with MA(17 nm)M exhibits a classical shape. In the others curves a S shaped effect is clearly visible, which justifies the poor efficiency of these OPVCs.
We used an equivalent electrical circuit model, to try to understand what is going on when the PET is substituted to glass as substrate.

4 Theory

The equivalent circuit used to interpret the I–V characteristics of solar cells consists of a photo-generator connected in parallel with a diode, which represents the I–V characteristics in the dark. This corresponds to an ideal model in absence of parasitic effects. However, in real OPVCs, it is necessary to introduce a series resistance, Rs, and a shunt resistance, Rsh. For such solar cells the mathematical description of this circuit is given by the following equation:

$$I = I_0\left(Exp\left[\frac{V - I\,R_S}{n\,k\,T}\right] - 1\right) + \frac{V - I\,R_S}{R_{Sh}} - I_{ph} \quad (1)$$

The Lambert W-function method has been used to determinate Rs, the series resistance, Rsh the shunt resistance, n the ideality factor of the diode and Iph the photo-generated current. The Lambert W-function is defined as the solution to the equation W(x) exp [W(x)] = x. The problem to be solved is the evaluation of a set of five parameters Rs, Rsh, n, Iph and Is in order to fit a given experimental I–V characteristics using a simple diode circuit. A good agreement between the experimental and theoretical fitted curves can be achieved only when the J-V curve does not exhibit a S-shaped effect i.e. only in the case of MAM with Ag thick of 17 nm (Figure 2, Table 2).

Technology Letters, Vol.2, No.3(2015) 5-11
ISSN: 2348-8131
Available online at www.technologyletters.us

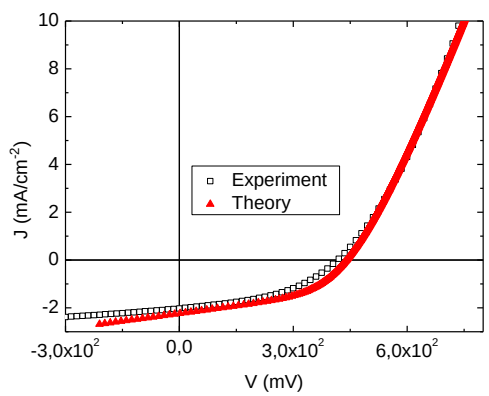

Figure 2: J–V characteristics under AM1.5 illumination of a solar cell using a MA(17 nm)M/Au/CuI anode structure (■) experimental and (▲) theoretical curves.

When the J-V curves exhibit a S-shaped effect, no agreement could be achieved, whatever the series and shunt resistance proposed. Such impossibility and the unrealistic n value show that the simple equivalent scheme used in this theoretical study cannot explain the experimental results obtained.

In the OPVCs, the process of hole collection is one of the main factors which control the electrical characteristics and the efficiency of the devices.

Anode/ABL	Main Junction					Back contact Junction			
	J_{ph} (mA)	J_{s1} (mA)	R_{s1} (Ω)	R_{sh1} (Ω)	n_1	J_{s2} (mA)	R_{s2} (Ω)	R_{sh2} (Ω)	n_2
MA(11 nm)M/CuI	3.42	$2.6x10^{-6}$	10	260	1.1	0.27	22	250	3
MA(11 nm)M/Au/CuI	3.2	$4.6x10^{-5}$	10	190	1.3	$5x10^{-2}$	2	120	1.7
MA(17 nm)M/CuI	3.16	$8.5x10^{-5}$	18	265	1.7				
MA(17 nm)M/Au/CuI	2.35	$4.5x10^{-5}$	22	450	1.65				

Table 2: Parameters calculated using a main diode and a back contact diode.

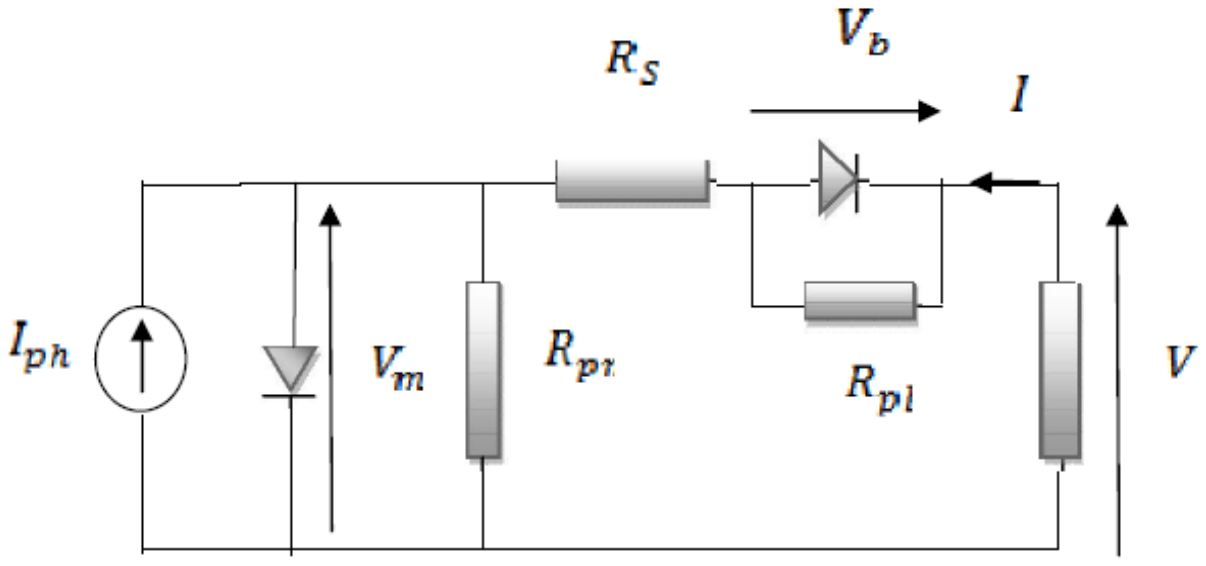

Figure 3: Equivalent electrical circuit of a cell exhibiting a S-shaped J-V curve.

Technology Letters, Vol.2, No.3(2015) 5-11
ISSN: 2348-8131
Available online at www.technologyletters.us

Therefore modifications of the anode properties can lead to dramatic modification of the performance of the solar cells. It was shown that the presence of S-shaped curves, which can be attributed to different phenomena, can be modeled through the introduction of a second diode of opposite polarity in the equivalent electrical circuit of the cell. Therefore, we have assumed the presence a back-contact barrier at the interface Anode/CuPc when the OPVC is submitted to one sun global AM 1.5 simulated solar illumination (Figure 3).
Assuming a thermoionic current at this interface, the hole current is:

$$Ib = -Ib_0 (\exp(-qVb/n_2kT) - 1) \quad (2)$$

With Ib_0 the saturation current, Vb the voltage across the back contact, k Boltzmann constant, and T temperature.
The current is negative because the polarity of the Anode/CuPc junction is opposite to the main CuPc/C_{60} junction.
Therefore the current-limiting effect, "S-shaped curve", is due to the back-contact barrier height. It occurs because the total current saturate at a value Jb_0 [10]. The value of Jb_0 is the current value where the J–V curve starts to show the S-shaped effect, i.e. when the slope of the curve starts to decrease while V continues to increases.
We suppose that, when a forward bias V is applied to the circuit, the voltage is divided between Vm across the main CuPc/C_{60} junction, Vb across the back-junction Anode/CuPc and IRs across the series resistance:
$V = Vm + Vb + IRs$.
Under illumination the current across the main junction is:

$$Im = Im_0 (\exp(qVm/n_1kT) - 1) - Iph + Vm/Rsh \quad (3)$$

and through the back contact it is:

$$Ib = -Ib_0 (\exp(-qVb/n_2kT) - 1) + Vb/R^b_{sh} . \quad (4)$$

Equating Eq. (3) with (4) yields:

$$Im_0 (\exp(qVm/n_1kT) - 1) - Iph + Vm/Rsh + Ib_0 (\exp(-qVb/n_2kT) - 1) - Vb/R^b_{sh} = 0 \quad (5).$$

The parameters Rs and Im_0, n, Rsh of the main diode are calculated in the region far from the saturation current Ib.
Then Eq. (5) can be solved. The obtained results are shown in Figure 4 and Table 2.

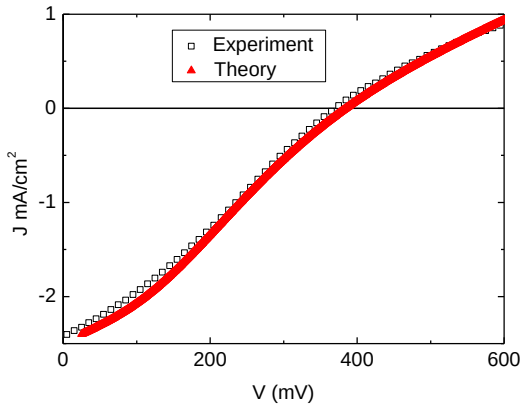

Figure 4: J–V characteristics under AM1.5 illumination of a solar cell using a MA(11 nm)M/CuI anode structure (■) experimental and (▲) theoretical curves.

A good agreement can be achieved between experimental and theoretical curves under light (Figure 4), which validates the hypothesis of the presence of a rectifying effect at the contact MA(11 nm)M/ABL.
One can see in Table 2 that, when the two diodes model is used, the estimated Rs values are of the same order of magnitude as those of anode using thick Ag film. The value of n is also realistic with the two diodes model. Therefore the introduction

of a back junction diode is a good interpretation of the interface MA(11nm)M/ABL/CuPc. It justifies their small fill factor.

There is not such S-shaped behaviour when the MA(11 nm)M structure is deposited onto a glass substrate [16], while the physical properties of the MA(11 nm)M structures are similar when deposited onto glass or PET substrates. The main differences between the MA(11 nm)M structures consist in the thickness and roughness of their substrates.

The glass substrate is thick of 1 mm, the PET substrate is thick of only 50 µm and while the rms of glass is lower than 0.5 nm, that of PET is 2.5 nm [7]. We have checked the substrate temperature at the end of the deposition process, the is 80 °C in the case of glass substrate and 110 °C in the case of PET substrate, due to its smaller thickness. Such temperature difference, added to the highest roughness of the PET can engender more easily paths favoured for silver diffusion, which can cause an important Ag migration toward the surface of the MAM structure during the deposit of the organic layers. Such Ag diffusion induces two main secondary effects. The fist consists in a significant increase of the sheet resistance of the MA(11 nm)M structure, due to the decrease of the real thickness of the Ag layer. The second consists in the decrease of the work function of the anode, since the work function of Ag is only 4.3 eV. The fact that the MA(11 nm)M structures become resistive after OPVC deposition justifies the appearance of the S-shaped curves. The resistive electrode implies the existence of large Rs, which hinders the charge transport at the interface and cause rapid reduction of FF. On the other hand this accumulative effect is amplified by the decrease of the work function (Φ_M) of the anode due to Ag diffusion towards the surface of the electrode since Φ_{MAg} = 4.3 eV. As the HOMO of CuPc is 5.2 eV, it does not allow achieving a good band matching between the anode and CuPc. The increase of the Ag layer allows preserving the conductivity of the structure even after OPVC deposition. However, if the sheet resistance of the MA(17 nm)M is now sufficiently small, the presence of Ag at the surface of the structure limits the band matching at the interface Anode/CuPc, which limits the performance of the OPVC. The insertion of an ultra thin layer of Au between the anode and the CuPc allows to improve the band matching [9] and to optimise the power conversion efficiency of the cells. Nevertheless the thickness of the Ag layer cannot overpass 17 nm, beyond there is a significant decrease of the transmission of the structures.

5 Conclusion

Using equivalent electrical circuits of a cell it is shown that the presence of S-shaped curves, which can be attributed to a too high value of the sheet resistance and too small work function of the anode, can be modeled through the introduction of a second diode of opposite polarity in the equivalent electrical circuit of the cell. For the future, in order to avoid these negative effect induce by the OPVC deposition, a thicker PET substrate will be used, while the substrate will be maintained at room temperature during the deposition process.

References

[1] L. Cattin, J.C. Bernède, M. Morsli, Physica Status Solidi a 210 (2013) 1047-1061.

[2] T-B. Song, N. Li, Electronics 3 (2014) 190-204.

[3] G. U. Kulkarni, S. Kiruthika, R. Gupta, KDM Rao, Current Opinion in Chemical engineering 8 (2015) 60-68.

[4] D. S. Hecht, L. Hu, G. Irvin, Advanced Materials 23 (2011) 1482-1513.

[5] C. Guillén and J. Herrero, Thin Solid Films 520, 1 (2011).
[6] L. Cattin, Y. Lare, M. Makha, M. Fleury, F. Chandezon, T. Abachi, M. Morsli, K. Napo, M. Addou, J. C. Bernède, Solar Energy Materials & Solar Cells 117 (2013) 103-109.
[7] T. Abachi, L. Cattin, G. Louarn, Y. Lare, A. Bou, M. Makha, P. Torchio, M. Fleury, M. Morsli, M. Addou, J.C. Bernède, Thin Solid Films 545 (2013) 438–444.
[8] M. Makha, L. Cattin, S. Dabos-Seignon, E. Arca, J. Velez, N. Stephant, M. Morsli, M. Addou, J. C. Bernède,
Indian Journal of Pure & Applied Physics 51 (2013) 569-582.
[9] L. Cattin, S. Tougaard, N. Stephant, S. Morsli, J. C. Bernède, Gold 44 (2011) 199-205.
[10] S. H. Demtsu and J. R. Sites, Thin Solid Films 510 (2006) 320-324.